Energy efficient active vibration control strategies using electromagnetic linear actuators

IOP Conf. Series: Journal of Physics: Conf. Series **1048** (2018) 012011 doi:10.1088/1742-6596/1048/1/012011

Energy efficient active vibration control strategies using electromagnetic linear actuators

Angel Torres-Perez, Ali Hassan, Stefan Kaczmarczyk, Phil Picton

The University of Northampton, St. George's Avenue, Northampton, NN2 6JD, United Kingdom

E-mail: angel.torresperez@northampton.ac.uk

Abstract. Energy efficient current control methods in electromagnetic linear actuators are required to minimize the electrical power requirements imposed by active vibration control strategies. In this paper an efficient bidirectional buck-boost converter is discussed in two scenarios: an active vibration isolation system and an active dynamic vibration absorber (ADVA) using a voice coil motor (VCM) actuator. An electrical analogous circuit of an experimental test platform is used as part of the simulation model. This test platform is based on a vibration shaker that provides the based excitation required for the single Degree of-Freedom (1DoF) vibration model under study. The proposed bidirectional non-isolated buck-boost converter can recover the energy when the VCM acts as a generator and store it for future use. Simulation results prove that this type of topology is far more efficient than linear amplifiers typically used in active vibration control. Within the context of slender structures, this efficient current control method improves the viability of using active vibration control in flexible structures such as beams.

Keywords: active DVA, bidirectional DC converters, switching power amplifier, buck-boost, voice coil motors

1. Introduction

A dynamic vibration absorber (DVA), or vibration neutralizer is a tuned spring-mass system which reduces or eliminates the vibration of a harmonically excited system. There are two types of DVAs depending on the need of external power to perform their functions. Passive DVAs do not require actuators and they cannot guarantee high vibration control performance for disturbance with various frequencies in general. However, active dynamic vibration absorbers (ADVAs) have sensors and actuators and are often considered when high vibration control performance is required for disturbance with various frequencies. The actuators of ADVAs are typically controlled using feedforward or close

loop controllers. DVAs has been extensively studied in building structures, as defence mechanism against earthquakes, to counter seismic movements and wind forces [1].
In this paper an electrodynamic actuator is used to modify and effectively control the mechanical stiffness and damping of a tuned mass damper. A feedforward controller is used to ensure the natural frequency of the vibration absorber tracks the disturbance main excitation frequency. As a result, the system has optimal performance throughout a large range of excitation frequencies. The feedforward controller requires accurate current control flowing through the electrodynamic actuator.
This study analyses an active DVA using an electrical analogous circuit model as discussed in [2]. This electrical analogy is used to set a comparison between a linear bridge current control amplifier and a switch mode power amplifier (class D) based on a bidirectional buck-boost converter.

2. Methodology

2.1. Active control rig

The experimental rig shown in Figure 1a. was built to test the concept of active control using an adjustable mass connected to a planar spring and one VCM actuator. Two motion sensors (piezoelectric accelerometers) are connected to the absorber mass and the shaker table respectively. Two electrical signals are recorded for VCM characterization that correspond to the current and voltage signals which are measured using one isolated differential voltage probe and one current probe respectively. The physical model which is a pictorial representation of the system under study is shown in Figure 1b.
The vibration model corresponds to a 1DoF with base excitation as shown in Figure 2.

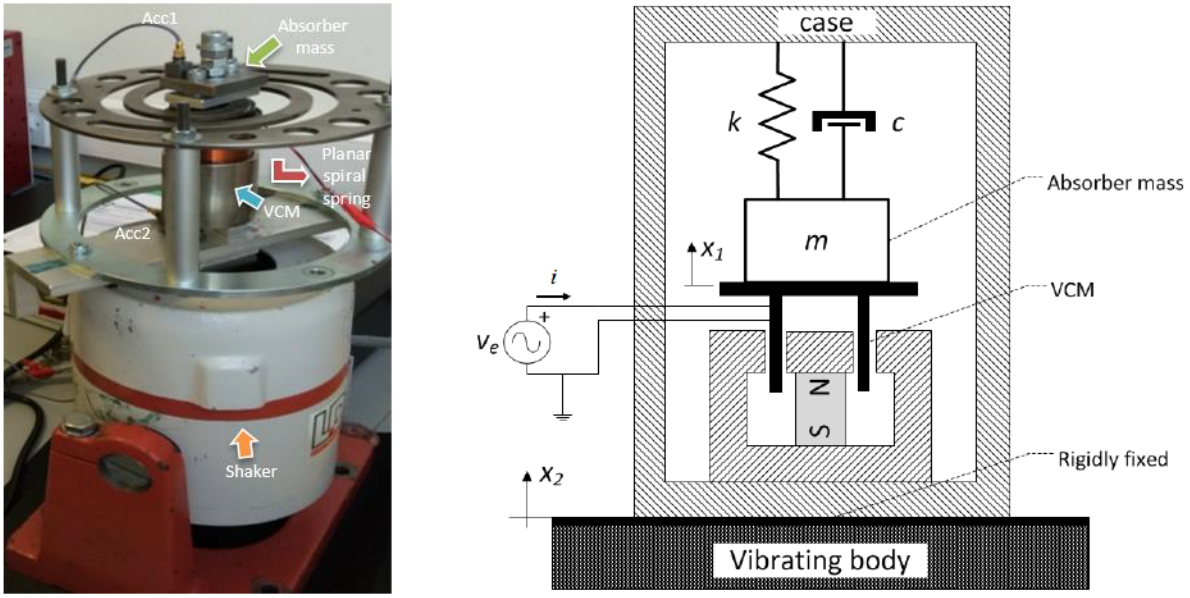

a) Experimental rig b) Physical model

Figure 1. Active vibration control rig [2]

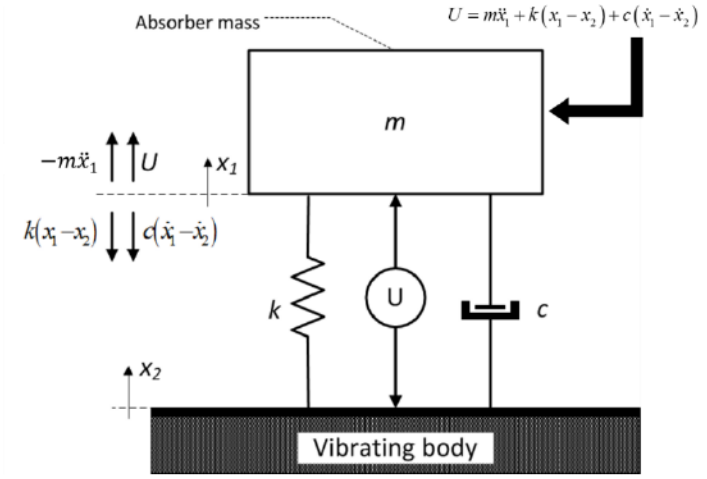

Figure 2. Active control vibration model with a generic actuator U (1DoF) [2]

2.2. Electromechanical Analogous Circuit

If the type of actuator is a Voice Coil Motor, the coupling equation between the electrical and mechanical system is due to Lorentz Force and Faradays's Law of Induction. The actuator mechanical force is proportional to actuator's current when there is a constant magnetic flux density in the VCM gap under all actuator stroke positions $N\frac{d\Phi}{dx} = cte$ as shown in (1).

$$F = \beta l \cdot i = \alpha_{VCM} \cdot i \tag{1}$$

The constant that multiplies the actuator current is referred as motor constant α_{VCM} . The definition is shown in (2) where α_{VCM} is the motor constant; N is the number of turns; β the magnetic flux density in the gap and l the length of the wounded wire.

$$\alpha_{VCM} = N\frac{d\Phi}{dx} = \beta l \tag{2}$$

The Back Electromotive Force is proportional to the total number of turns and actuator speed as shown in (3).

$$E = -N\frac{d\Phi}{dt} = -N\frac{d\Phi}{dx}\frac{dx}{dt} = -\alpha_{VCM}\dot{x} \tag{3}$$

A possible circuit representation that couples the mechanical system and electrical side uses a gyrator and it is shown in Figure 3. The governing differential equations for this circuit are obtained by applying Kirchoff's Voltage Law in loop1 and loop 2 as shown in (4).

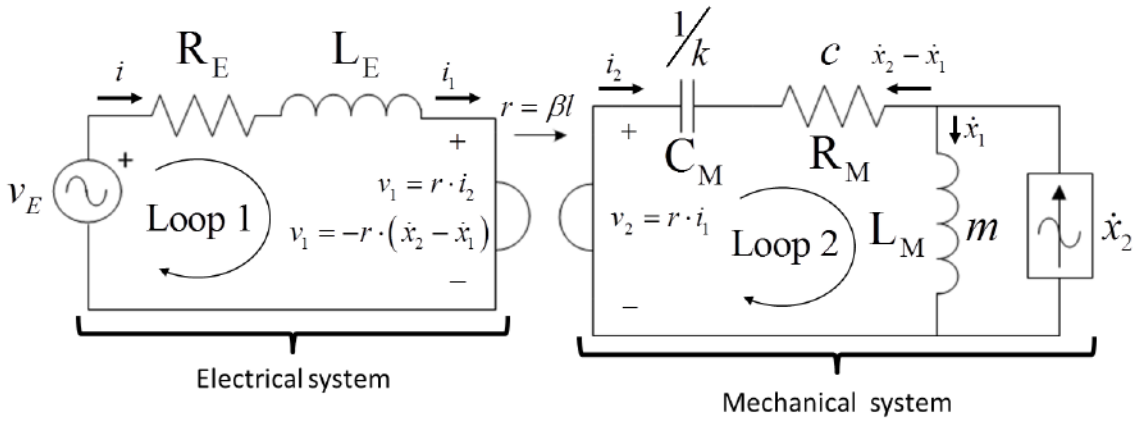

Figure 3. 1DoF active control rig with VCM (Type II)

$$\begin{aligned} V_E - R_E \cdot i - L_E \cdot \frac{di}{dt} - v_1 = 0 \quad | \; i = i_1 \\ v_2 + k(x_2 - x_1) + c(\dot{x}_2 - \dot{x}_1) - m\ddot{x}_1 = 0 \quad | \; i_2 = -(\dot{x}_2 - \dot{x}_1) \end{aligned} \tag{4}$$

These equations could be represented as a function of the currents in the electrical and mechanical sides of Figure 3 as shown in (5). The relationship between electrical and mechanical quantities is shown in Table 1.

$$r = \beta l = \alpha_{VCM} \begin{cases} V_E - R_E \cdot i - L_E \cdot \dfrac{di}{dt} + r \cdot (\dot{x}_2 - \dot{x}_1) = 0 \\ r \cdot i + k(x_2 - x_1) + c(\dot{x}_2 - \dot{x}_1) - m\ddot{x}_1 = 0 \quad | \; U = r \cdot i = \alpha_{VCM} \cdot i \end{cases} \tag{5}$$

Table 1. Interpretation of electrical and mechanical quantities

Electrical Quantity	Mechanical Analog II (Force Voltage)
Voltage, e	Force, f
Current, i	Velocity, v
Resistance, R	Friction, B
Capacitance, C	Compliance, 1/K (Inverse spring constant)
Inductance, L	Mass, M

A better circuit representation that considers damping due to eddy currents in the VCM when there is an open circuit across the terminals is shown in Figure 4. The circuit shown in Figure 4 provides a trend that is in good agreement with experimental results when the VCM terminals are under open and closed circuit conditions respectively. The circuit values are shown in Table 2. A further discussion about the derivation of this circuit is shown in [2] . It has been observed that the damping due to eddy currents it is also affected by the actuator stroke and current flowing through the main coil.

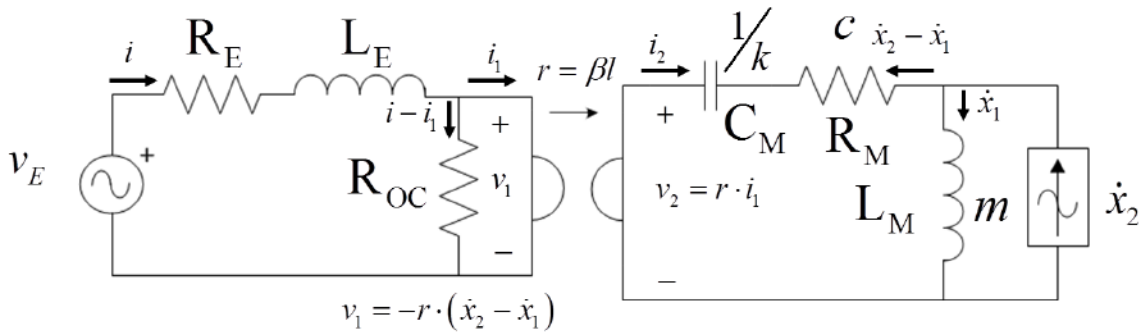

Figure 4. 1DoF active control rig with VCM

Table 2. Circuit values

Parameter	m	c	k	$f_0 = \frac{1}{2\pi}\sqrt{\frac{k}{m}}$	$\alpha_{VCM} = r$
Value	432.4	0.5 Negligible	42.167	49.7	7.4
Unit	[g]	[Ns/m]	[kN/m]	[Hz]	[N/A]

Parameter	L_E	R_E	R_{OC}	C_M	L_M	R_M
Value	4.1	3.3	9.78	23.71	0.4324	0.5
Unit	[mH]	[Ω]	[Ω]	[μF]	[mH]	[Ω]

3. ACTIVE CONTROL LAWS (ADVA)

The force U introduced by the actuator using the feedforward controller as shown in (6) must remove the damping of the system *c* and modify the natural frequency of the absorber to be the same as the main harmonic component of the vibration signal [3].

$$U(j\omega) = V(j\omega)\left(c + j\omega\underbrace{\left(m - \frac{k}{\omega^2}\right)}_{\alpha}\right) = V(j\omega)\left(c + \frac{j}{\omega}\underbrace{\left(\omega^2 m - k\right)}_{\gamma}\right) \tag{6}$$

$$V(j\omega) = j\omega\cdot\left(X_1(j\omega) - X_2(j\omega)\right)$$

Where $V(j\omega)$ is the relative speed of the absorber mass with respect to the vibrating body in the frequency domain. The absorber tuning could be shifted to the harmonic excitation frequency ω by introducing a force proportional to actuator relative position $(x_1 - x_2)$ times a constant of magnitude α or a force proportional to actuator relative acceleration $(\ddot{x}_1 - \ddot{x}_2)$ times a constant of magnitude γ. Thus, two possible gains, one proportional to acceleration (α) and the other proportional to position (γ) could be defined relative to the natural resonant frequency of the absorber mass ω_0. These gains are shown in (7) and (8).

$$\alpha = \left(m - \frac{k}{\omega^2} \right) \xrightarrow{\omega_0 = \sqrt{\frac{k}{m}}} \alpha = m\left(1 - \left(\frac{\omega_0}{\omega} \right)^2 \right) \tag{7}$$

$$\gamma = \left(\omega^2 m - k \right) \xrightarrow{\omega_0 = \sqrt{\frac{k}{m}}} \gamma = m\left(\omega^2 - \omega_0^2 \right) \tag{8}$$

The force U, exerted by the VCM is the current times the motor constant (r). Therefore, the actuator force is controlled by the current flowing through the VCM terminals. A current controlled power amplifier is needed for this task. The stiffness in the mechanical side of Figure 4. could be modified by selecting a current *i* that is proportional to the relative position times the position gain over the motor constant γ/r. The effective mass in the mechanical side of Figure 4 could be altered by selecting a current that is proportional to the relative acceleration times the acceleration gain over the motor constant α/r.

4. CURRENT CONTROL AMPLIFIER

The current flowing through the VCM is adjusted using a power amplifier. The feedforward controller requires an amplifier with a fast-current loop minimizing any delays in the actuator force. This precision amplifier is typically implemented with a class AB amplifier with low distortion level, negligible output voltage/current ripple and poor efficiency (50%). The main drawback of this power amplifier is that the dissipated power depends on output power factor. This type of amplifier is quite inefficient when driving low impedance and reactive loads. All the reflected energy from reactive components and back EMF is consumed dissipating heat. A block diagram of a class AB amplifier with current control is shown in Figure 5a and in a bridge configuration in Figure 5b.

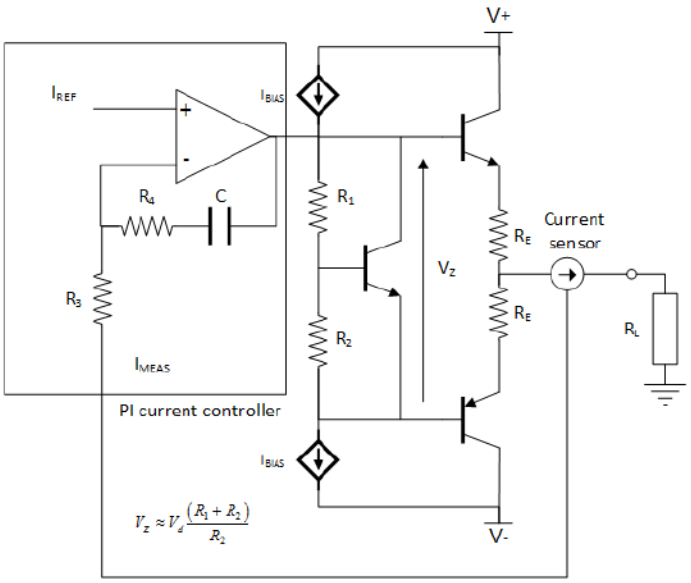

Figure 5a. Linear amplifier (class AB), push-pull output stage

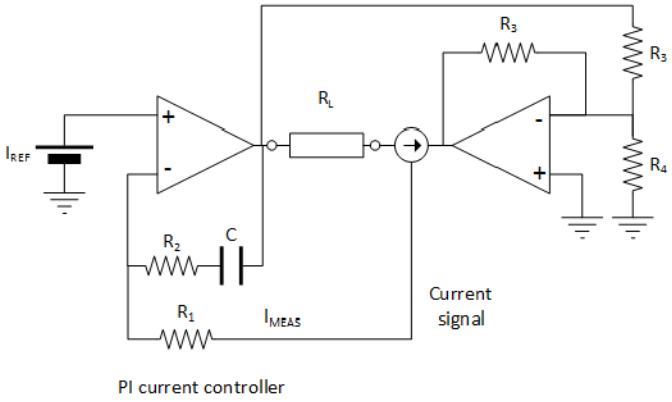

Figure 5b. Linear amplifier (class AB) in a bridge configuration

In this paper, an efficient current controlled class D amplifier controls the current through the VCM. The circuit topology in Figure 6a resembles a synchronous buck converter [4] and it is sometimes referred as bidirectional buck-boost converter [5]. A small signal model and average state space model is shown in [5]. The steady state analysis assumes a constant average current through the inductor, hence the volt-second balanced condition in one switching cycle is met and the ratio between the output and input voltages could be obtained as shown in (9) where Ts is the switching period and D is the duty cycle.

$$(V_s - V)DT_s = (V_s + V)(1-D)T_s \rightarrow \frac{V}{V_s} = D - (1-D) = 2D - 1 \tag{9}$$

Thus, the DC voltage gain is a linear function of the duty cycle D as shown in Figure 6b. For $D > 0.5$ the output voltage is of positive polarity, while for $D < 0.5$ it is of negative polarity. The switch S could be implemented using two transistors allowing a bidirectional current flow.

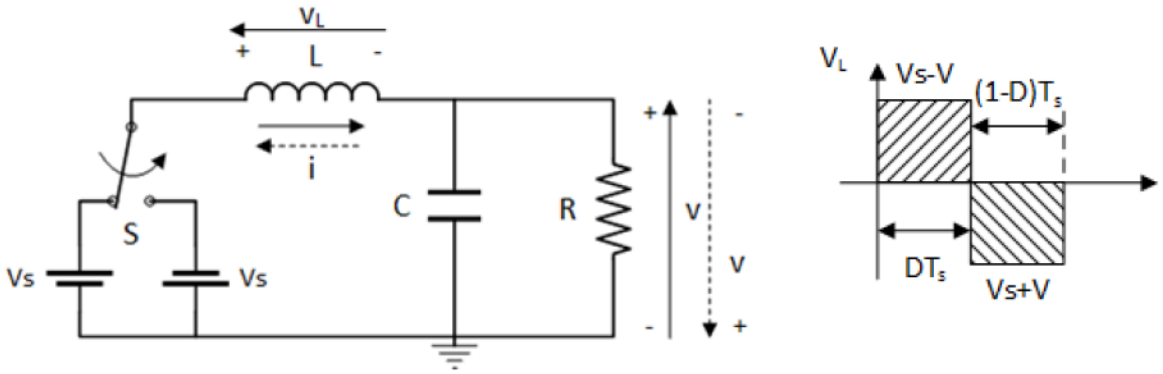

Figure 6a. Switching amplifier derived from the buck converter

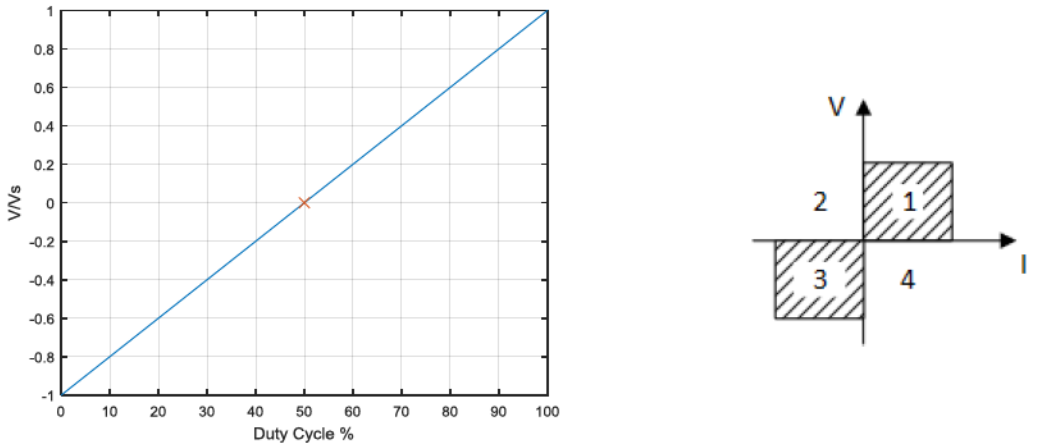

Figure 6b. Ratio between the output and input voltages (two quadrant operation)

The hardware implementation of the switch S in Figure 6a, corresponds to a power amplifier in a half bridge configuration as shown in Figure 7a. A single power supply implementation requires four transistors according to the bridge circuit in Figure 7b. The PWM output of the PI current controller in Figure 7c is the control signal for the transistors of the class D amplifier. The PWM signal is generated comparing the output signal of the PI controller against a high frequency sawtooth signal.

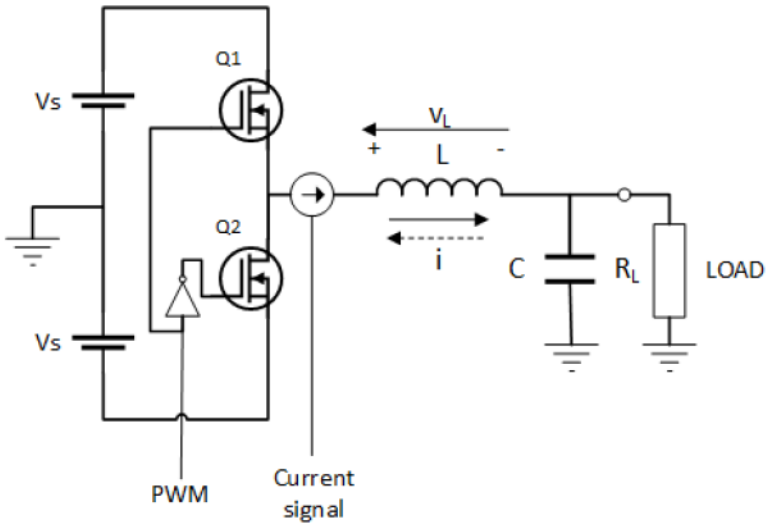

Figure 7a. Class D amplifier (half bridge)

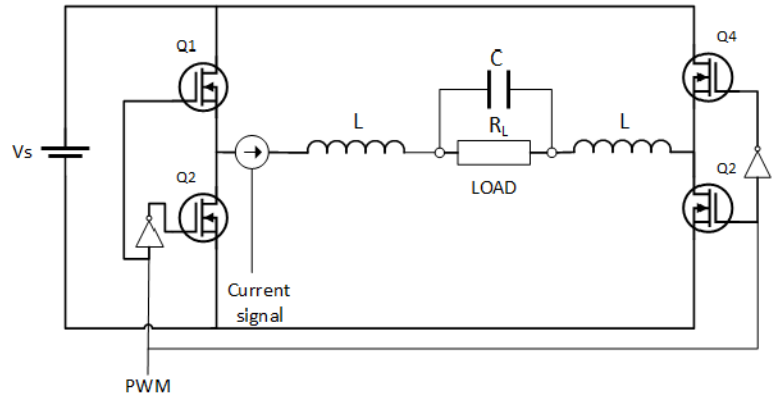

Figure 7b. Class D amplifier (full bridge)

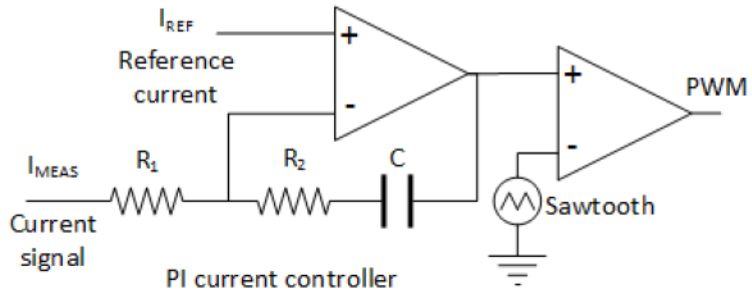

Figure 7c. PWM signal generation (current control)

5. Simulation results

The full bridge implementation of the switching amplifier with the analogous circuit as the load was simulated in PSIM. The low pass differential LC filter was designed with a cut-off frequency of 230Hz which is much lower than the PWM frequency. The inductor L is 1mH and the capacitor 470μF. The equivalent single ended filter shown in Figure 8 is used for calculating the cut off frequency and quality factor calculations of the differential filter. The base excitation (shaker table) was assumed to be a constant amplitude sinusoidal speed signal of 0.1m/s of peak amplitude and a frequency of 50Hz.

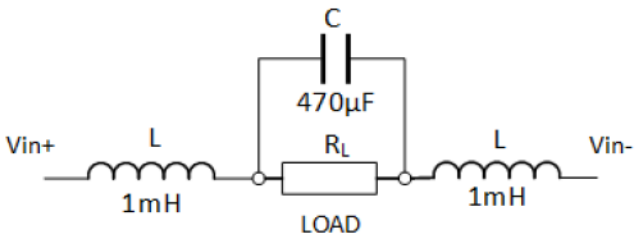

Figure 8. Differential filter and it is Single-Ended Equivalent

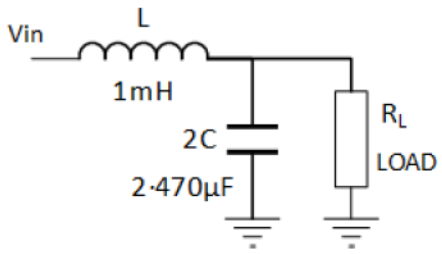

A frequency response analysis of the switching amplifier shown in Figures 9a-b was conducted in open loop around the operating point (D=50%). The gyrator block in Figure 9b was implemented with two current controlled voltage sources. The ac sweep was conducted by varying the duty cycle around the operating point (signal injection). The open loop response of the inductor current as a function of the duty cycle for different frequencies is shown in Figure 9c. The system is stable, and the phase margin is 90°.

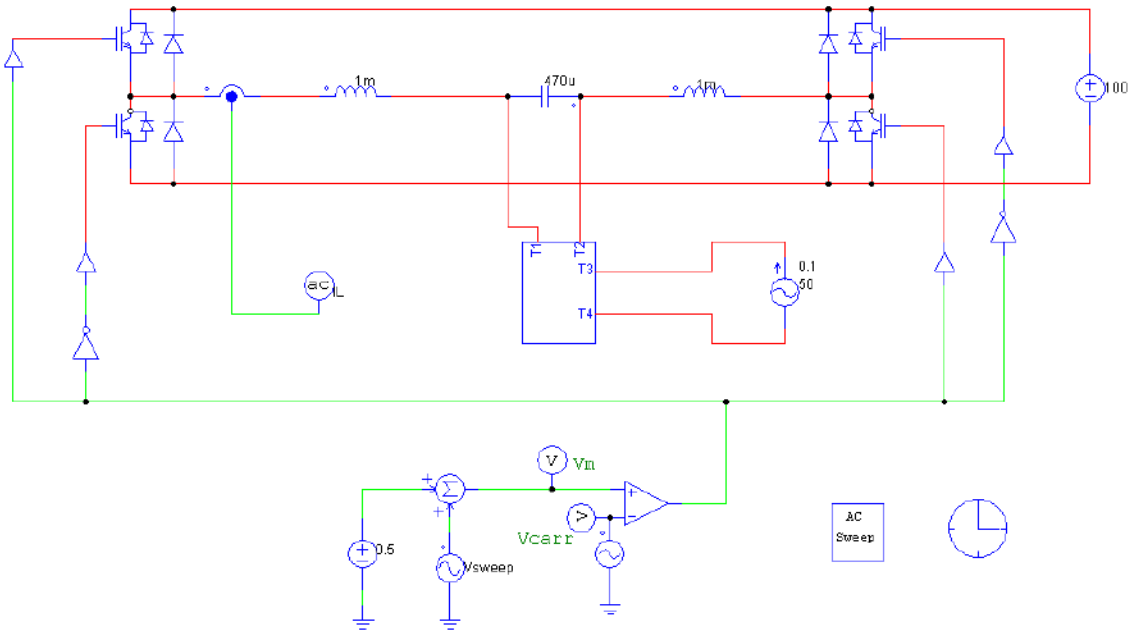

Figure 9a. Class D amplifier with analogous circuit as the load

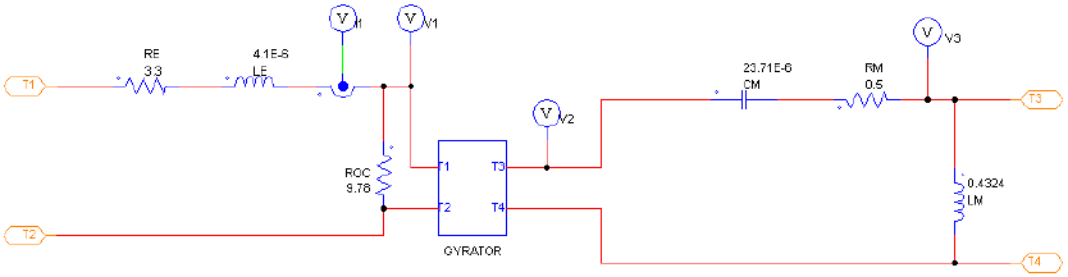

Figure 9b. Analogous circuit implementation (load)

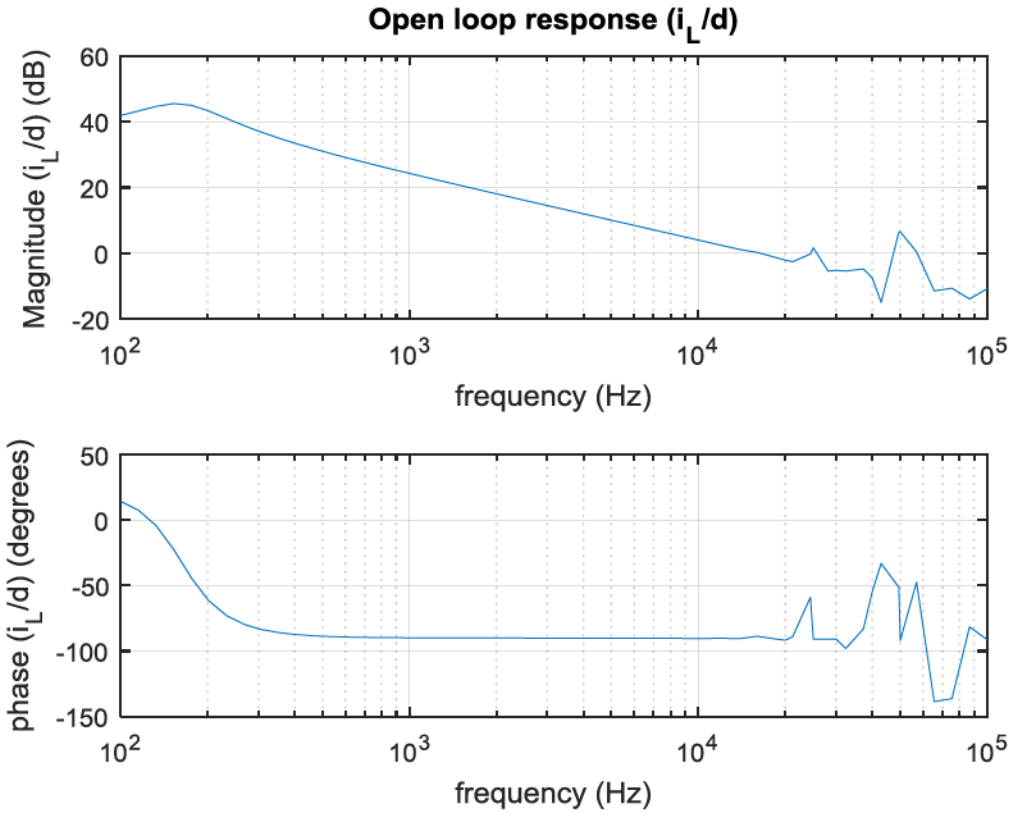

Figure 9c. AC Sweep analysis (open-loop, duty cycle 50%)

Closed loop response was analysed using the transient analysis shown in Figures 10a-c. Current control was performed using a PI regulator $G(s) = k\,(1 + sT) / (sT)$ with a gain of 8 and a time constant of 100µs. The PWM signal is generated comparing the output of the PI controller against a sawtooth signal frequency of 50Khz and peak to peak voltage of 1V. The saturation block after the PI regulator limits the range of the duty cycle from 0 to to 95% (it corresponds with an output between 0 and 0.95V). In Figure 10b, a transient analysis was performed to measure power requirements and the differential voltage across the load. Figure 10c represents the measured and reference load currents when the reference current signal is a sine wave of 50Hz and 2A of peak voltage with 1A of DC offset. The simulation results in Figure 10b do not consider the on resistance of the switches, the resistance of the output filter and wire resistances. Therefore, the power conversion efficiency is ideal, and all the input power is transferred to the load. A linear amplifier (AB type) will never reach this efficiency because the transistors are operating in the linear region.

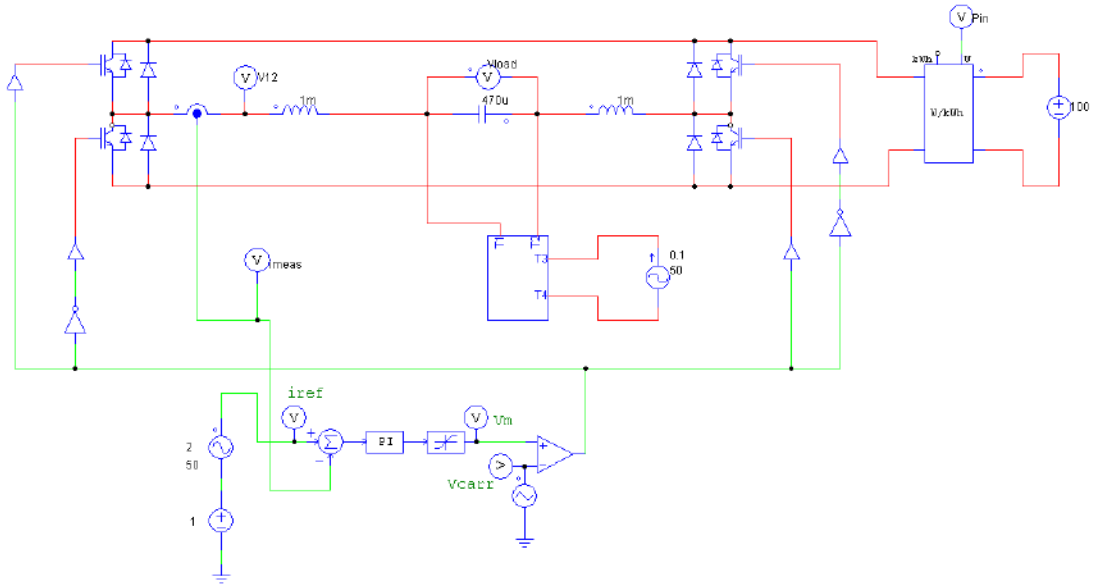

Figure 10a. Transient analysis (PI current controller)

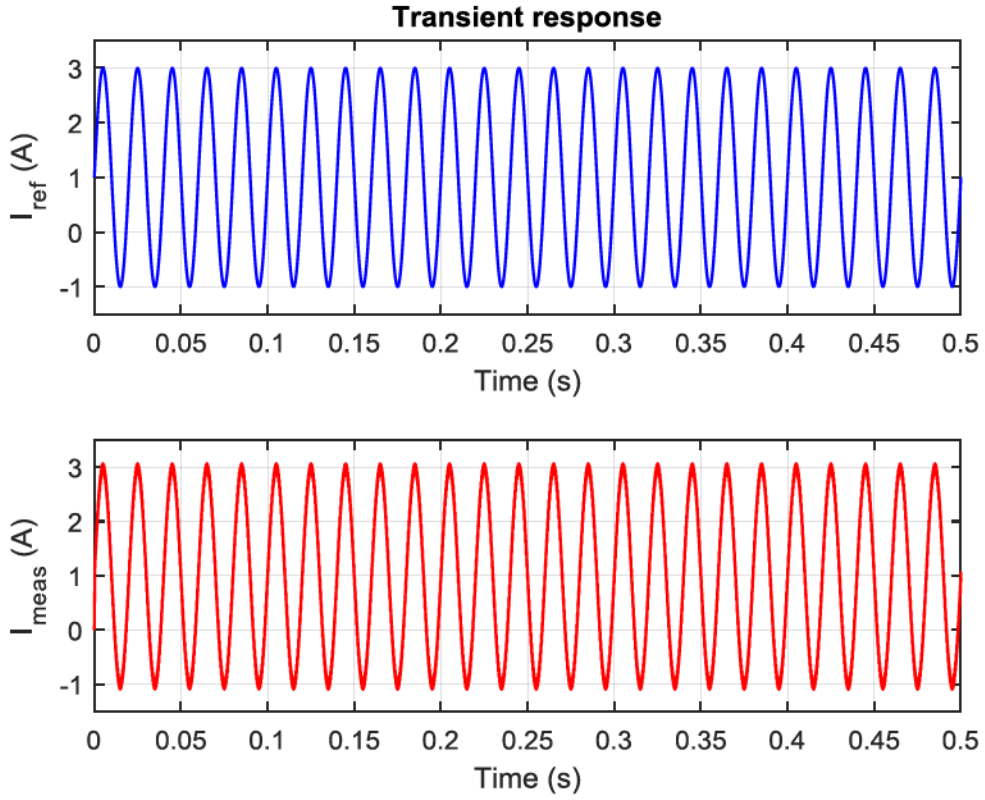

Figure 10b. Transient results (PI current controller). Reference and measured currents.

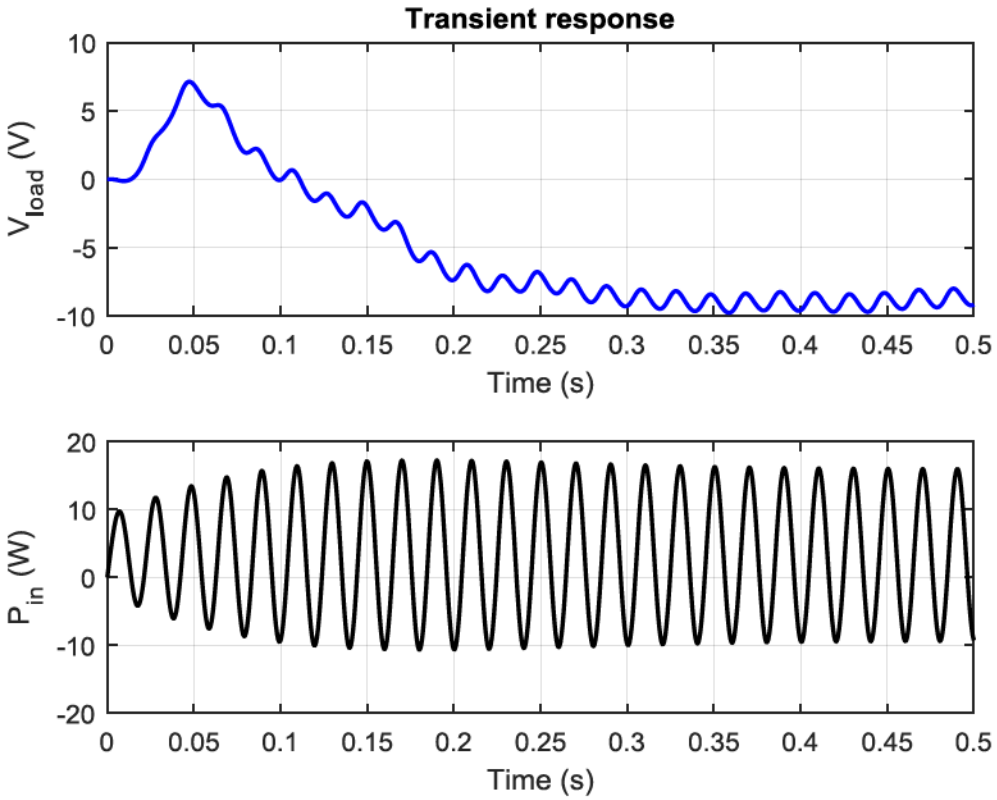

Figure 10c. Transient results (PI current controller). Voltage across the load and power input requirements.

6. Conclusions

The proposed electromechanical analogous circuit is quite useful for studying the dynamics and efficiency of power amplifiers in active vibration control systems. Standard circuit simulation software could be used for tuning the real system.
The proposed current control amplifier shows high efficiency (the losses are largely determined by the ratio of the load resistance to the total DC loop resistance which is the sum of the on resistance of the MOSFETs, wire resistances (including the output filter) and current sense resistor if used, and the load resistance.
The bandwidth of the current control amplifier is quite high which is desired for successfully implement the feedforward controller. The main drawback when compared to the class AB amplifier is the output current ripple. This output current ripple could be minimized increasing the switching frequency and the L value in the output filter.
Simulation results indicate that the proposed current controlled Class D amplifier is an efficient VCM driver for active vibration control.

7. References

[1] Samali, B., Al-Dawod, M., Naghdy, F. *Active Control of Cross Wind Response of 76-Story Tall Building Using a Fuzzy Controller*, Journal of Engineering Mechanics, 130 (4) (2014), pp. 492-498
[2] Perez, A., Hassan, A., Kaczmarczyk, S., Picton, P., Active vibration control using mechanical and electrical analogies, J. Phys.: Conf. Ser. 721 012013
[3] R.F.A. Marques, D.A. Rade, S.S. Cunha, Jr., Assessment of an Active Dynamic Vibration Absorber, IMAC XIX - 19th International Modal Analysis Conference (2001), pp, 32-36.
[4] Cuk, S., Erickson, R.W., A conceptually new-high frequency switched-mode power amplifier technique eliminates current ripple, in Proc. Fifth Nat. Solid-State Power Conversion Conf., (1978), pp. G3.I-G3.22.
[5] Zhang, J., Bidirectional DC-DC Power Converter Design Optimization, Modelling and Control, PhD Dissertation (2008), Virginia Polytechnic Institute